Journal of Applied Research and Technology

www.jart.icat.unam.mx

Journal of Applied Research and Technology 22 (2024) 167-179

Original

Cotton fabric surface treatment by plasma-deposited hexamethyldisilazane thin films

W. Alali[a]* • Z. Saffour[a] • S. Saloum[b]

[a]*Spinning and Textile Department- Petrochemical Faculty- Al Baath University- Homs- P.O.B. 77, Homs, Syria*
[b]*Atomic Energy Commission of Syria, Physics Department, P.O.B. 6091, Damascus, Syria*

Received 09 13 2023; accepted 10 24 2023
Available 04 30 2024

Abstract: In the realm of fabric finishing, achieving the best wettability in cotton fabric is often a desired outcome. To accomplish this, a plasma-enhanced chemical vapor deposition (PECVD) system was used to deposit Hexamethyldisilazane (HMDSN) thin films onto cotton fabric for two different durations: 15 and 30 minutes. Various fabric properties were evaluated to determine the effectiveness of the treatment, including wettability, surface morphology, chemical structure, the effect of deposition on fabric stiffness, and the film fastness on the abrasion and washing. These properties were assessed using SEM, FTIR, and Martindale tester. Results indicated that both treatment durations improved the fabric's wicking ability and reduced the deformation of the fibers after the abrasion. However, the film did not have a good fastness on abrasion and washing.

Keywords: Cotton fabric, deposition, HMDSN, PECVD, wettability

*Corresponding author.
E-mail address: weaam6140@gmail.com (W. Alali).
Peer Review under the responsibility of Universidad Nacional Autónoma de México.

1. Introduction

Fabric finishing is a pivotal aspect of the textile industry, as it enhances the quality of the fabric and imbues it with specific functional properties (Choudhary et al., 2018; Zouari et al., 2021). However, traditional techniques such as sol-gel processing and polymerization require the immersion of fabric in chemical solutions that can be detrimental to the environment, impact fabric comfort, and result in excessive water and chemical waste. Thus, it is imperative to explore alternative eco-friendly methods for fabric finishing (Ibrahim & Eid, 2020; Naebe et al., 2022).

As for more sustainable practices, the search for eco-friendly methods of fabric finishing is underway (Samanta et al., 2021; Xu et al., 2020). The plasma technique presents a promising option, as it can be utilized on a range of materials, including polymers and fabrics. This process encompasses cleaning, etching, activating, and depositing to prime the surfaces for subsequent finishing stages (Mohamed & El-Halwagy, 2021; Murbat et al., 2018).

Plasma is a remarkable form of matter found abundantly in the universe, consisting of ions, electrons, and free radicals, and is considered the fourth state of material (Atta et al., 2019; Su et al., 2019). One of its most fascinating qualities is its highly efficient processing, making it a quicker and more energy-saving alternative to traditional methods. Moreover, this eco-friendly and clean process requires no solutions, avoiding water and chemical waste (Kim et al., 2021; Zaidy et al., 2019).

The versatility of plasma technology is vast and improves various properties of fabrics such as wettability, static electricity, cleaning, shrinkage resistance, UV resistance, abrasion resistance, flame retardancy, dye absorption, and even medical engineering applications (El-Sayed & Hassabo, 2021).

In the realm of fabric finishing, cotton fibers hold immense significance. Before finishing processes, achieving the best wettability is a critical component of the pretreatment process. Through cleaning the cotton fabric to eliminate impurities and enhance its wettability, a uniform finish with consistent coloration (whether dyed or printed) and superior fastness properties can be achieved. This indispensable step is necessary to guarantee the utmost quality of finished cotton products (Cavaco-Paulo et al., 2019; Colombi et al., 2021).

Plasma-enhanced chemical-vapor deposition, or PECVD, is a sophisticated technique that employs a gas treatment using a molecule monomer. This monomer is vaporized and interacts with active species, such as electrons, ions, and free radicals, within the plasma, leading to fragmentation. This process causes a unique film deposition onto the substrate surface within the plasma reactor, known as plasma polymerization. Moreover, this technique is efficient, requiring only minimal amounts of precursor materials and consuming minimal energy (Saloum et al., 2019a; Saloum et al., 2019b Saloum et al., 2020a; Saloum et al., 2020b).

The utilization of organosilicon monomers via the PECVD technique has become prevalent across numerous fields as a treatment material. Among the most widely employed monomers are HMDSO and HMDSN. Typically, when the PECVD technique is applied to these organosilicon compounds, it yields a transparent film with a chemical structure of $SiO_xC_yH_z$ or $SiN_xC_yH_z$ (Jaritz et al., 2021; Rosace et al., 2010). Although HMDSO polymeric films have been utilized in the treatment of various fabrics (Ibrahim & Eid, 2020; Prado et al., 2022; Rosace et al., 2010; Zouari et al., 2021), HMDSN has yet to be used in fabric finishing, while it was used in other fields, where silicon organic thin films were prepared from HMDSN with different feed gases (Nitrogen and Argon), and the formed thin films had a good wettability and promising characteristics for sensing humidity of air and sensing ammonia gas (Saloum et al., 2020a).

In addition, plasma polymerized thin films using HMDSN/nitrogen and HMDSN/argon compounds were prepared, these films had a wettability property and could be used in industrial applications such as electronics, electrics, and other fields (Kodaira et al., 2015; Kodaira et al., 2012).

In this research paper, we delve into the application of the RF plasma-enhanced chemical vapor deposition (PECVD) method in depositing a plasma-polymerized thin film composed of HMDSN onto cotton fabric. The goal of this study is to evaluate the effects of this treatment on the fabric's wettability, as well as its chemical and morphological characteristics, and its effect on the stiffness of the fabric.

2. Materials and methods

Materials

Hexamethyldisilazane (HMDSN: $C_6H_{19}Si_2N$) (98% purity from Sigma-Aldrich) was used as an organosilicon monomer precursor due to its availability, transparent liquid state, safety, and ease of use. Argon and helium (99.999% purity) were used as the feed gas and HMDSN vapor carrier gas, respectively.

The deposition process was performed on three types of substrates:

- 1/1 plain woven 100 % cotton fabric with a grammage of 180 g/m^2, a thickness of 0.23 mm, and a density of 33 and 18 yarn/cm for warp and weft, respectively. Fabric samples with dimensions 200 × 65 mm^2 were used in the treatment.
- A quartz microbalance crystal was used as a sensor to determine the weight of the deposited film due to the piezoelectric effect of the quartz material.
- Silicon wafers (n-type <100>, 500 µm thickness) were used for the thickness measurement of the deposited film by SEM.

Before plasma treatment, the fabric underwent bleaching and desizing with NaOH and H_2O_2 to eliminate contaminants. It was then neutralized with acetic acid and washed with distilled water. After that, it was air-dried for 24 hours.

Experimental procedure

The experiment utilized an innovative setup known as a low-pressure hollow cathode discharge system, specifically the plasma consults GmbH PlasCon HCD-L 300 (Fig. 1), which is well explained elsewhere (Saloum et al., 2019a). This configuration comprises two tubes, namely the cathode and anode, which have coaxial holes that produce 30 plasma jets. The process began by evacuating the reactor chamber, which measures 50 x 50 x 50 cm^3, to a base pressure of 5 x 10^{-4} mbar with the aid of two pumps, namely the Alcatel 2063 C2 and Alcatel RSV 301B. RF power at 100 W and 13.56 MHz was then applied to initiate the treatment process.

The evaporation system employed in the experiment comprised a liquid mass flowmeter, Lintec-LM-2100A, and an evaporator, Lintec-VU 410, heated to 70°C. HMDSN vapor was subsequently conveyed to the reactor chamber via helium gas through a 70°C heating line.

A stainless-steel holder, positioned at 45 mm below the source, was used to secure the sample under the plasma source. The deposition process was conducted twice, first for 15 minutes, and then for 30 minutes, at room temperature with flow rates of Ar (20 sccm), He (40 sccm), and HMDSN vapor (16 sccm), while maintaining a constant working pressure of about 0.12 mbar. It is noteworthy that 1 sccm is equivalent to 1 standard ml/min.

3. Results and discussion

3.1. Morphological analysis

The surface morphology of the samples and film thickness were analyzed using a scanning electron microscope (Vega II XMU Teskan SEM) at up to 10,000x magnification.

Fig. 2 highlights the surface morphology of the samples, whereas Fig. 2 (a, b) displays the surface fibers of the untreated sample. Meanwhile, Fig. 2 (c, d) and Fig. 2 (e, f) exhibit the deposited film on the 15 min and 30 min treated samples, respectively. Fig. 3 outlines the thickness of the deposited film on the treated samples, with measurements of 18 and 54 nm for 15 min and 30 min treated samples, respectively.

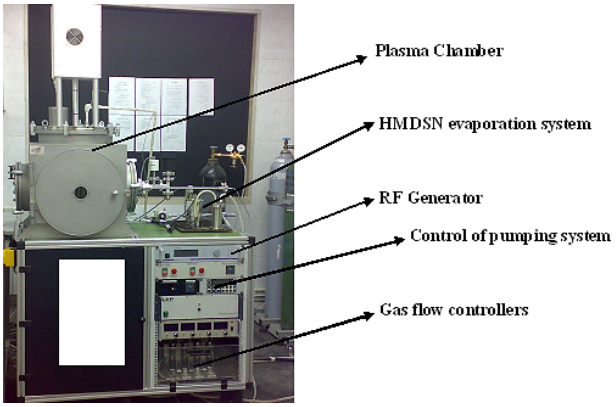

(a)

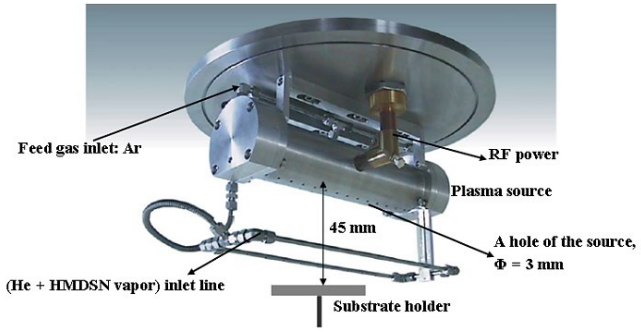

(b)

Figure 1. (a) Plasma deposition system of HMDSN thin films. (b) View of the plasma source, feed gas inlet, Hexamethyldisilazane (HMDSN) vapor inlet, and the position of the substrate holder inside the plasma chamber.

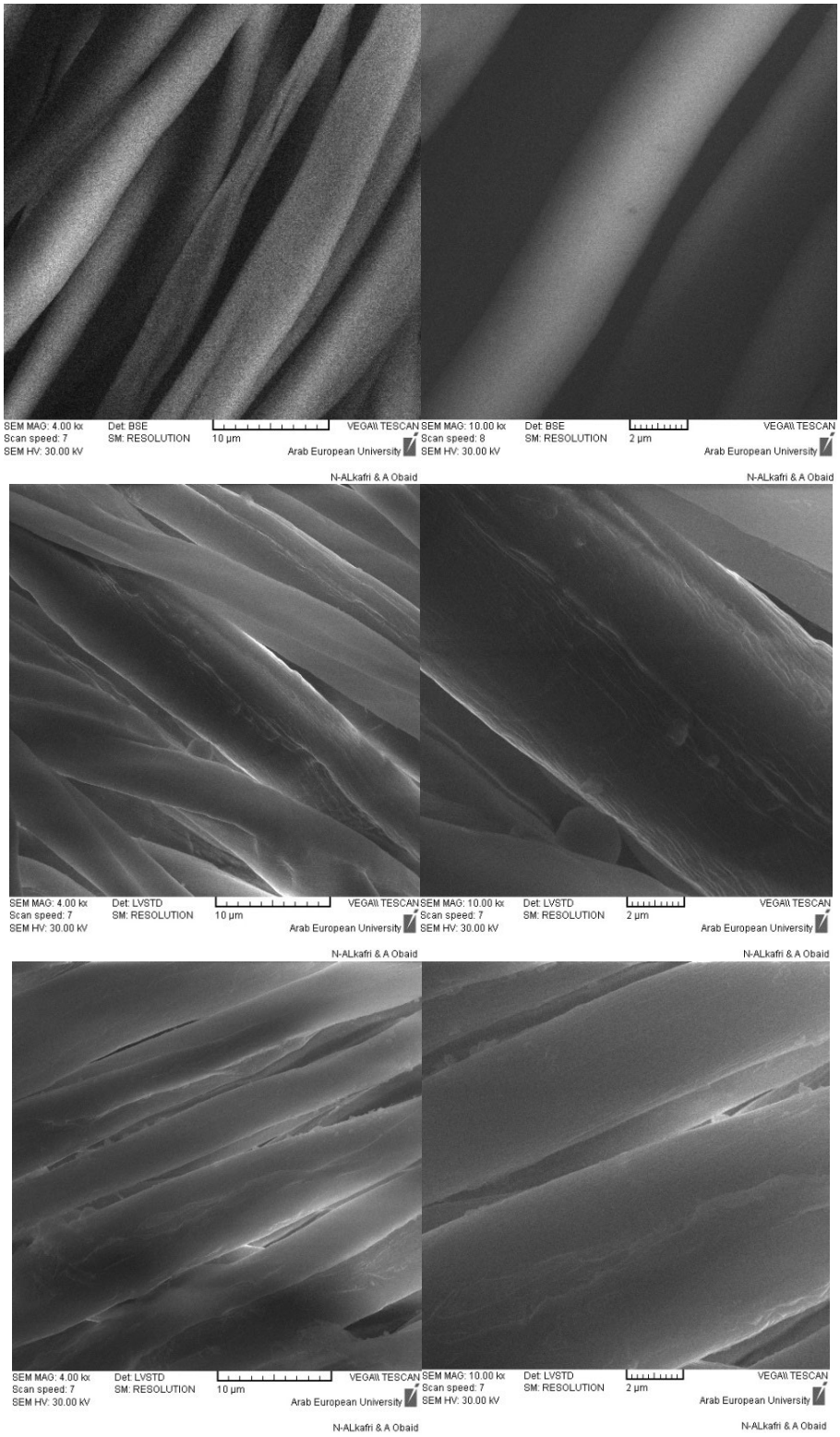

Figure 2. Surface morphology of the samples: (a, b) untreated sample, (c, d) 15 min treated sample, (e, f) 30 min treated sample with magnification 4000× in (a, c, e) and 10000× in (b, d, f).

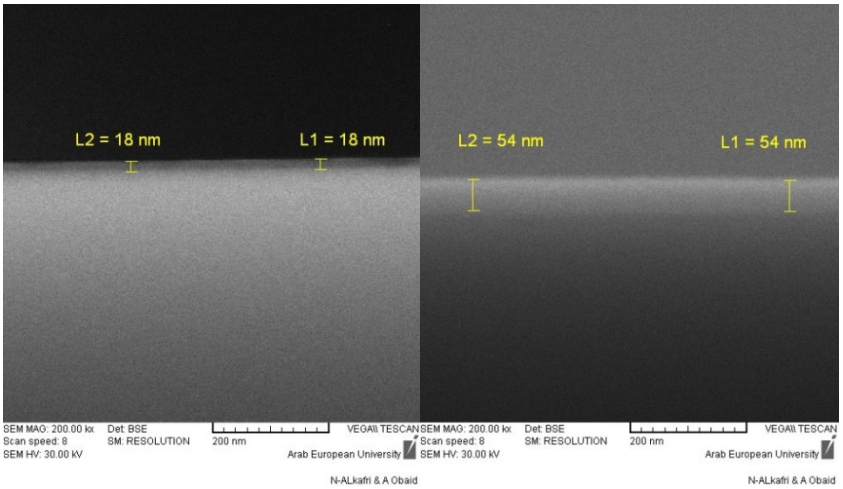

Figure 3. The thickness of HMDSN film on silicon wafers: (a) at deposition time 15 min, and (b) at deposition time 30 min with magnification 200000×.

The weight of the deposited film was determined using the quartz microbalance crystal which responds to the deposition process by a change in the oscillation frequency (Δf) (Saloum et al., 2019a), and this change can be monitored and converted to a change in mass (Δm) by Sauerbrey relationship Eq. (1) (Saloum et al., 2019a):

$$\Delta f = \frac{(f0^2.\Delta m)}{(\rho.\,N.\,A)} \quad (1)$$

where: *f*0 is the resonant frequency of the quartz crystal (about 6.0 MHz), ρ is the density of quartz (2.65 g.cm^{-3}), N is the frequency constant of quartz (1.67 × 105 Hz.cm), A is the area of the deposited crystal, and d is the thickness of the deposited film. Table 1 shows the properties of the deposited film.

As the duration of deposition increases, so does the thickness of the film. Yet, the slight increase in the film weight with the increase in the deposition period can be attributed to the low density of the deposited HMDSN film that is described in Eq. (2) (Sohbatzadeh et al., 2019):

$$\Delta m = A.\,d.\,\rho \quad (2)$$

Table 1. The properties of HMDSN deposited film.

Deposition period	Weight of the deposited film on the quartz crystal (μg)	Thickness (nm)
15 min deposition	12.55	18
30 min deposition	16.58	54

3.2. Wettability analysis

To gauge the wicking ability, we adhered to DIN 53824 (1997) standard. A 25 x 200 mm^2 strip of the sample was suspended vertically, with one end dipped approximately 3 mm into distilled water. To clarify the results, we introduced a solubilized dye and monitored the water level within the strip over a period of time. The procedure lasted for 30 seconds, with three measurements taken for each sample, and the mean value was calculated.

The results of the wicking experiment are presented in Fig. 4, revealing that the treatment has improved the fabric's ability to absorb water. This improvement is due to the formation of polar groups on the fabric's surface. As a result of the plasma process, the monomer undergoes breakdown into smaller chemical components and free radicals through inelastic collisions. These ions then break down the side groups and hydrogen bonds present at the ends of the cellulose chain when they penetrate the polymeric film. The free radicals generated during this process become trapped in the structure and react with oxygen in the atmosphere, resulting in the creation of polar groups within the film structure (Kodaira et al., 2015).

3.3. Chemical structure analysis

To analyze alterations in the surface chemical structure of plasma-treated samples and identify the absorption bands and functional groups in both untreated and treated samples, attenuated total reflectance Fourier Transform Infrared Spectroscopy (ATR-FTIR Thermo Nicolet 6700) was employed. The samples were precisely subjected to 64 scans within the wavenumber range of 400 - 4000 cm^{-1}.

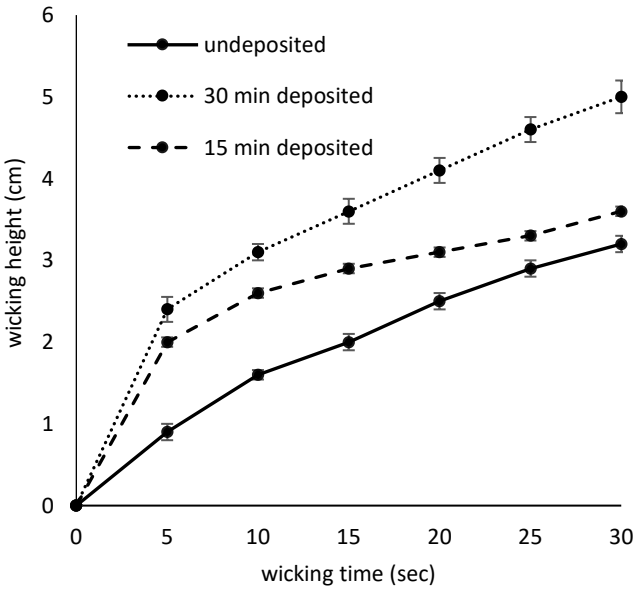

Figure 4. Water wicking height.

Table 2 provides peak assignments for cellulose in untreated and treated samples, while Table 3 displays the peak assignments for the HMDSN-deposited film in treated samples, and in Fig. 5, the spectrum of the samples analyzed by FTIR is presented.

The Hexamethyldisilazane molecule is composed of a silazane group (Si-N-Si) with three methyl groups (-CH_3) attached to each silicon atom. Fig. 5 displays the distinguished bonds in cellulose present in untreated and treated samples, which include C-O, C-H, and -OH. The treated samples also contain bonds belonging to the HMDSN deposited film, such as Si-C, Si-O, Si-H, C-H, C=O, N-H, C-N, and Si-NH-Si .

It is important to note that the absorption band at 1030 cm^{-1}, related to C-O bonds in the untreated sample, increases after treatment due to Si-O stretching bonds from the HMDSN deposited film. The appearance of C=O bonds is explained by the incorporation of atmospheric oxygen and moisture into the film structure after formation .

Functional groups like -NH_2, C=O, and C-N contribute to an increase in wettability. Regarding Si-H, it only appears in the 30 min treated sample, not in 15 min treated sample. This may be due to the FTIR technique's limited sensitivity in detecting nanometric chemical changes.

Table 2. FTIR peak assignments for cellulose in the samples.

Peak	Assignment	Wavenumber (cm^{-1})			Reference
		Untreated sample	15 min treated sample	30 min treated sample	
1	C-O asymmetric stretching	1030, 1110, 1160	1030, 1110, 1160	1030, 1100, 1160	(Sohbatzadeh et al., 2019)
2	C-H bending	1430	1420	1420	(Nandiyanto et al., 2019)
3	C-H symmetric stretching	2850	2860	2860	(Kozak et al., 2018; Sohbatzadeh et al., 2019)
4	-OH symmetric stretching	3270, 3340	3340, 3370	3310, 3360	(Prado et al., 2022)

Table 3. FTIR peak assignments for HMDSN deposited film in the treated samples.

Peak	Assignment	Wavenumber (cm^{-1})		Reference
		15 min treated sample	30 min treated sample	
1	Si-C stretching	665	660	(Mourya et al., 2018)
2	Si-O stretching	1030	1030	(Kozak et al., 2018)
3	C-H bending	1420	1420	(Nandiyanto et al., 2019)
4	C-N	1550	1550	(Kozak et al., 2018)
5	N-H bending	1650	1640	(Nandiyanto et al., 2019)
6	C=O	1730	1730	(Saloum et al., 2019b)
7	Si-H	-	2110	(Kozak et al., 2018)
8	C-H symmetric stretching	2860	2860	(Kozak et al., 2018; Sohbatzadeh et al., 2019)
9	N-H stretching	3450	3400, 3450	(Guruvenket et al., 2012; Kozak et al., 2018)
10	Si-NH-Si	3560	3550	(Guruvenket et al., 2012)

3.4. Stiffness test

This test was conducted following ASTM D1388-96 (2002) standard. The sample with defined dimensions was placed on a flat surface and a graduated ruler was positioned above it, as depicted in Fig. 6. The ruler was gradually pushed forward, propelling the sample until its bent end met the line inclined at a 41.5° angle from the horizontal. Six to eight seconds later, the measurement on the ruler was taken, which indicated the bending length of the sample. Finally, Eq. (3) was used to calculate the stiffness:

$$\mathrm{G} = \mathrm{W} \times C^3 \times \mathrm{K} \tag{3}$$

Where: G is the stiffness of the sample (g.m), W is the grammage of the sample (g/m^2), C is the bending length (m), and K is a constant, it is as in Eq. (4):

$$\mathrm{K} = \frac{\cos\left(\frac{1}{2}\theta\right)}{8\tan\theta} \tag{4}$$

Where θ is the bending angle. Based on the findings presented in Table 4, the treatment has resulted in a minor increase in the fabric's stiffness. This outcome may be because solely the outermost layer of fibers is treated during the deposition procedure. It should be emphasized that this approach to finishing fabrics frequently yields excessive weight gain and decreased comfort (Zouari et al., 2021).

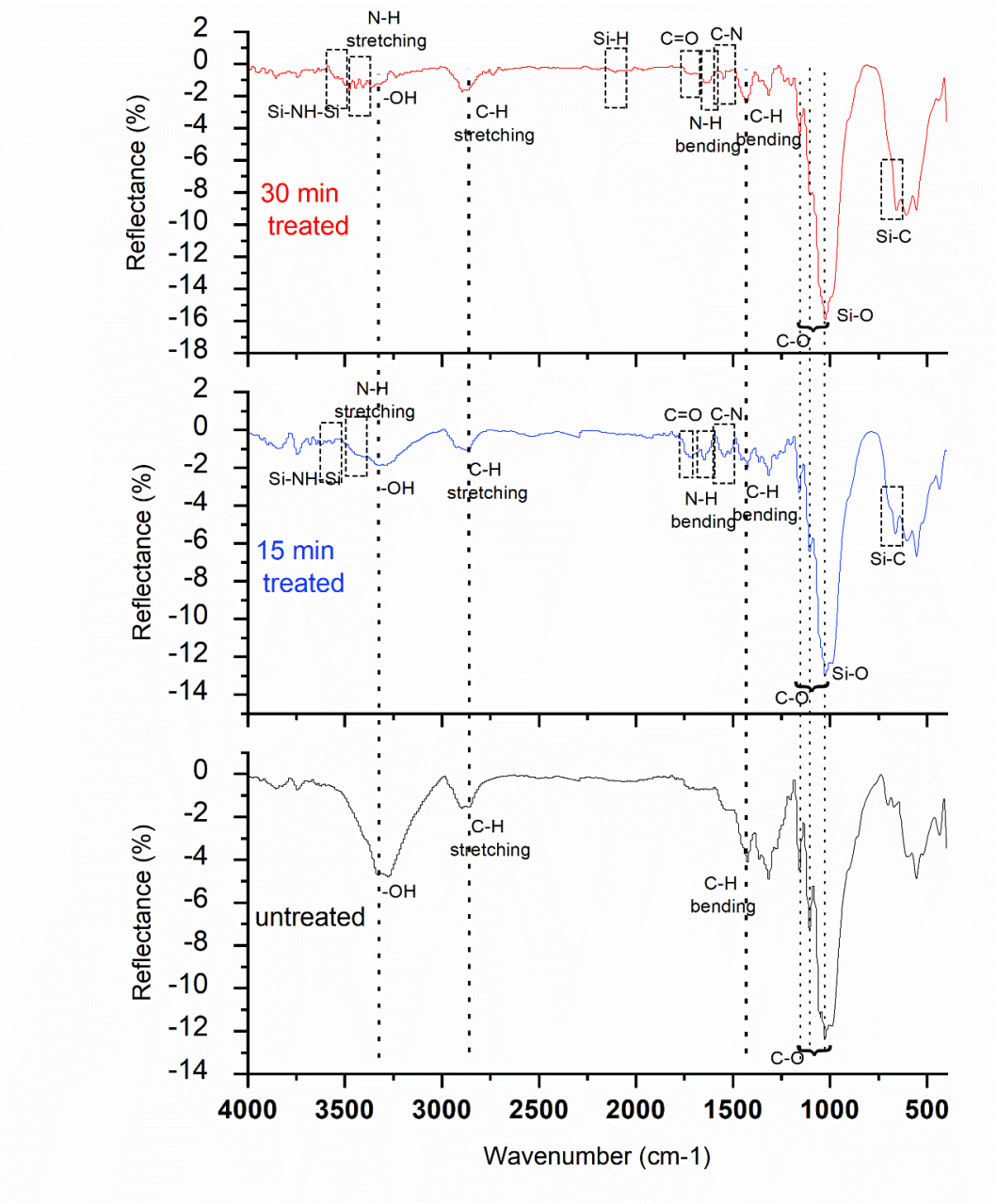

Figure 5. FTIR spectrum of the samples.

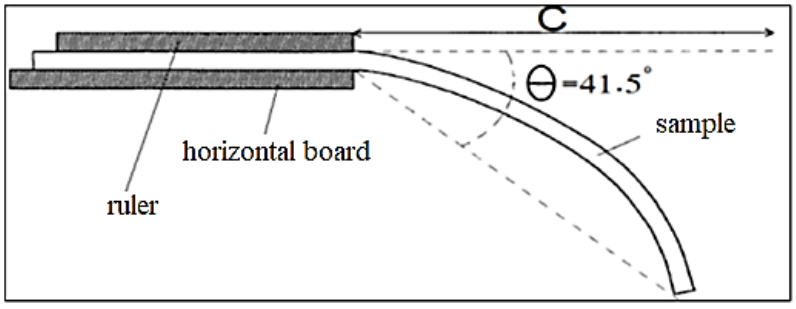

Figure 6. Stiffness test for samples.

Table 4. The properties of HMDSN deposited film.

Sample	Bending length (cm)	Stiffness (g.m)
Untreated sample	3.4	0.0009347
15 min treated sample	3.7	0.001204
30 min treated sample	4	0.001522

3.5. The film fastness to abrasion

The abrasion resistance of the film was evaluated using Martindale device by DIN EN ISO 12947-3 standard, where the circular sample (diameter 38 mm) was mounted and clamped in a sample holder, and after being subjected to a specified load (9 kPa), rubbed against a standard fabric with a translational motion.

The weight loss of samples was calculated for 500, 750, and 1000 cycles by weighting the sample before (W1) and after the cycles of rubs (W2) according to Eq. (5):

$$\text{weight loss}(\%) = \ (W1 - W2)/W1 \ \times 100 \qquad (5)$$

Fig. 7 displays the weight loss of the samples after undergoing the abrasion test. The findings reveal that weight loss progressively increases with the number of Martindale cycles. As it was noted, the treatment resulted in decreased weight loss, thanks to the thin PECVD coating that was applied to the sample, which helped to decrease the weight loss of the sample.

The results are like those of Rosace et al. (2010), who reported an improvement in abrasion performance when treating cotton fabric with Hexamethyldisiloxane through the PECVD process for 12 minutes. However, they did not treat the fabric for an extended period.

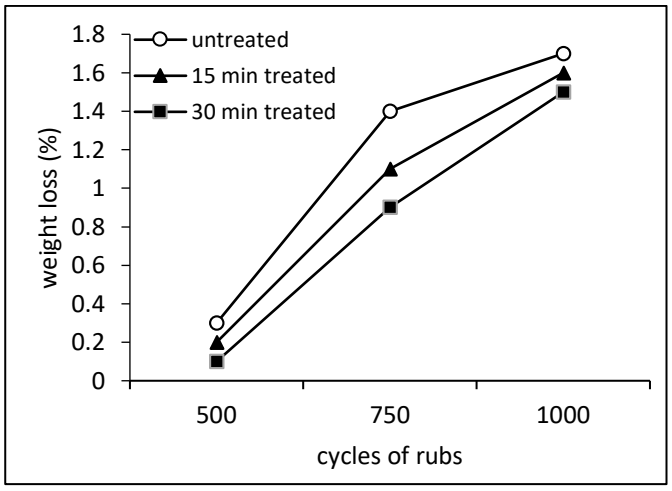

Figure 7. Weight loss of samples after the abrasion test

In addition to the Martindale test, the samples were also analyzed for changes in the chemical structure and morphology of the surface of the fibers after 1000 cycles of rubbing.

Fig. 8 illustrates FTIR spectra of samples after 1000 cycles of rubbing, showing a decrease in HMDSN absorption bands for both treated samples (15 and 30 minutes). This suggests that a little portion of the deposited film has been removed after 1000 cycles of rubbing, indicating weak bonds between the deposited film and the cellulose chain.

Fig. 9 shows the fibers' surface morphology after 1000 cycles of rubbing, where it can be noted that the untreated sample has significantly deformed after the abrasion, while the deposition process has reduced the fiber deformation after the abrasion even after 1000 cycles of rubs.

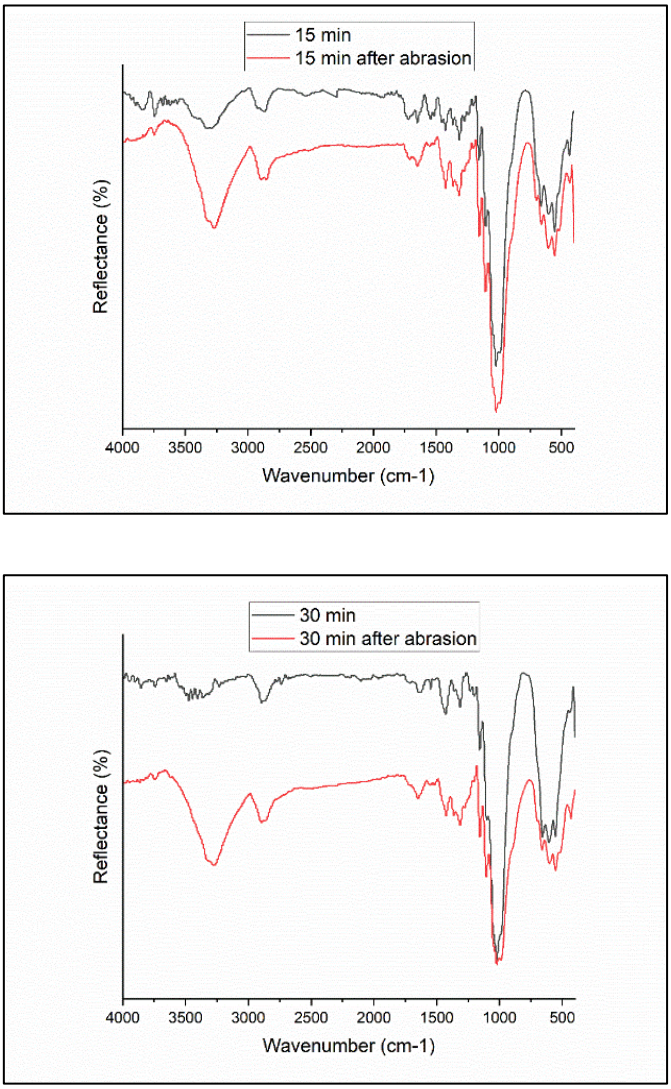

Figure 8. FTIR spectra for a) 15 min treated sample, and b) 30 min treated sample before and after 1000 cycles of rubs.

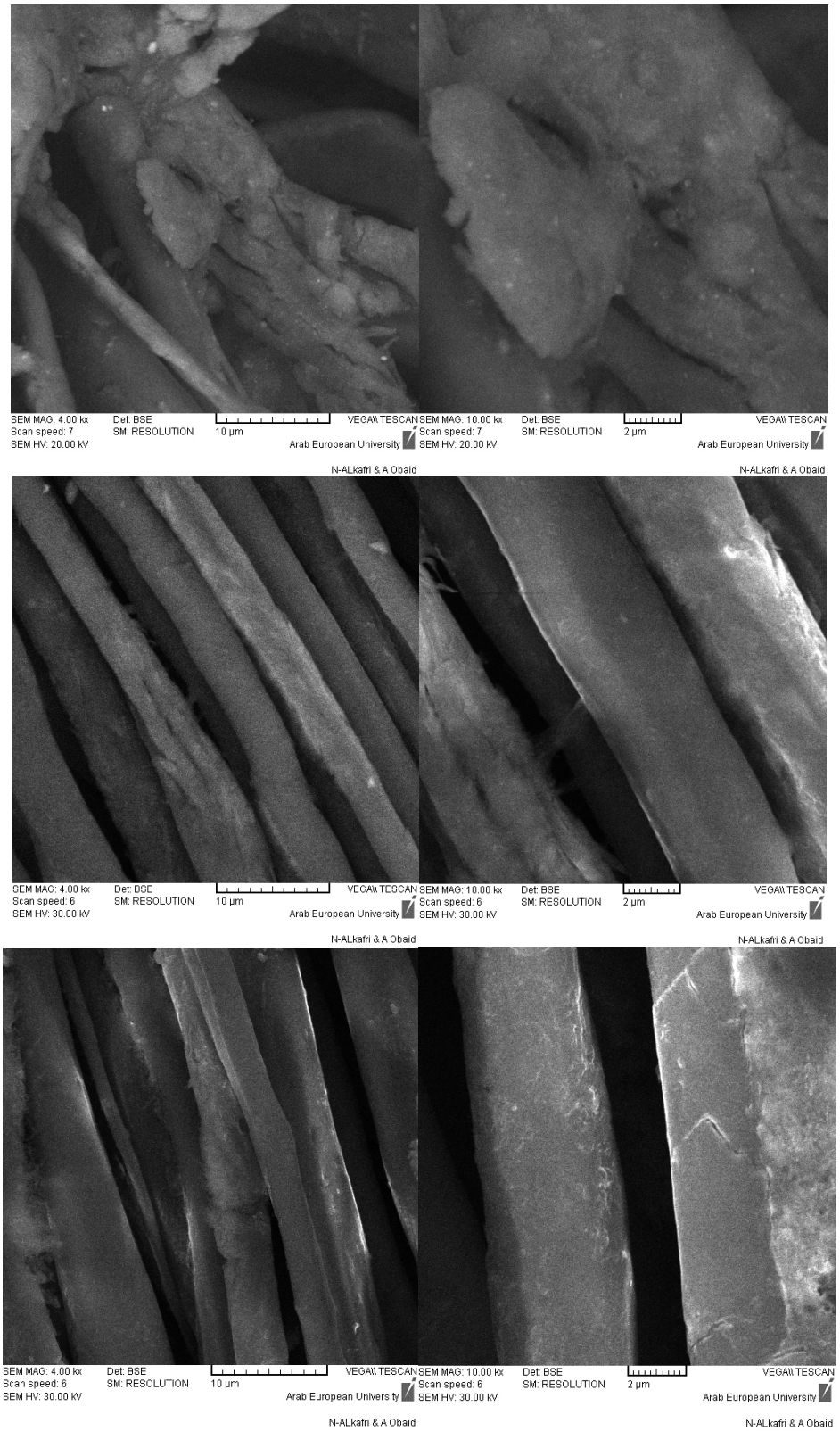

Figure 9. SEM images for: (a, b) untreated sample, (c, d) 15 min treated sample, and (e, f) 30 min treated sample after 1000 cycles of rubs.

3.6. The film fastness to washing

ISO 105 C01 was used for the washing test to analyze the film's resistance to washing, following a 30 min washing process at 40 ± 2°C, adhering to ISO 105 C01 standard. The samples were then left to dry in an open-air environment. To assess their washing fastness, the chemical composition of the samples was examined using FTIR analysis, which can be seen in Fig. 10.

The HMDSN absorption bands exhibited a decrease in both treated samples, while the -OH absorption bands showed an increase after the washing process. This suggests that a portion of the film deposited had been removed during washing. Based on this observation, it is presumed that the deposited film was not attached to the cellulose chain through covalent and ionic bonds.

4. Conclusion

During this study, a layer of HMDSN was expertly applied to cotton fabric using PECVD method, which lasted for 15-30 minutes. The outcome of this treatment process was truly remarkable, as it significantly enhanced the fabric's wettability, as evidenced by its superior wicking ability. Further examination of the fabric samples via SEM imagery revealed a thin film coating the surface fibers, with analysis indicating alterations in the film's weight and density. FTIR analysis confirmed that silicon and nitrogen were successfully incorporated into the surface of the treated fabric. Additionally, it could be seen that the fabric exhibited a slight increase in stiffness following the treatment process.

So, the deposition of HMDSN in a brief time on cotton fabric using the PECVD technique has significantly introduced the best wettability and the abrasion resistance of the fabric, which is suitable for various laboratory and industrial purposes. Moreover, this technique is highly economical as does not necessitate massive quantities of treatment materials and energy. The deposition process has reduced the deformation of the fibers after the abrasion. Nevertheless, the FTIR spectra obtained after washing and abrasion testing exhibit partial removal of the deposited film, indicating a requirement for additional research to enhance the bond between the film and the fabric.

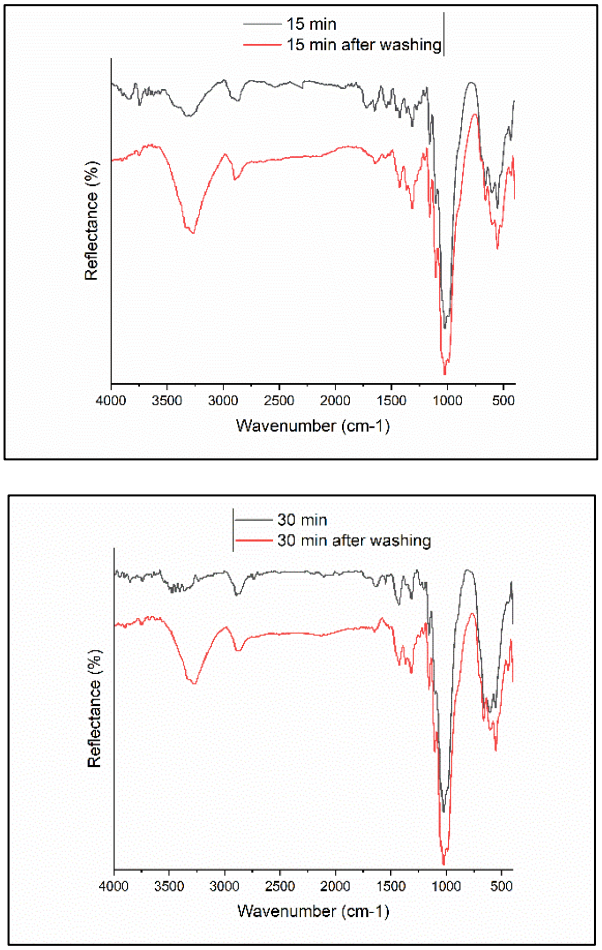

Figure 10. FTIR spectra for a) 15 min treated sample, and b) 30 min treated sample before and after washing.

Conflict of interest

The authors do not have any type of conflict of interest to declare.

Acknowledgement

The authors contributed to the design and implementation of the research, the analysis of the results, and the writing of the manuscript.

The authors would like to thank the general director of the Atomic Energy Commission of Syria, and the head of the Department of Spinning and Textile at Petrochemical College at Al-Baath University for their support and cooperation.

Funding

The authors have received financial help from the head of Al-Baath University – Homs - Syria. The recipient is the Ph.D. student Weaam Alali; the grant number is 1211- 26/4/2022.

References

Atta, A., Al Haideri, H., & Murbat, H. H. (2019). Influence of cold atmospheric plasma on Acinetobacter baumannii. *Baghdad Science Journal*, *16*(1), 151-161. https://doi.org/10.21123/bsj.2019.16.1(Suppl.).0151

Cavaco-Paulo, A., Nierstrasz, V. A., & Wang, Q. (2019). *Advances in Textile Biotechnology*. Woodhead Publishing.

Choudhary, U., Dey, E., Bhattacharyya, R., & Ghosh, S. K. (2018). A brief review on plasma treatment of textile materials. *Adv. Res.* Text. Eng, 3(1), 1-4.

Colombi, B. L., Valle, R. D. C. S. C., Valle, J. A. B., & Andreaus, J. (2021). Advances in sustainable enzymatic scouring of cotton textiles: evaluation of different post-treatments to improve fabric wettability. *Cleaner Engineering and Technology*, *4*, 100160. https://doi.org/10.1016/j.clet.2021.100160

El-Sayed, E., & Hassabo, A. G. (2021). Recent advances in the application of plasma in textile finishing (A Review). *Journal of Textiles, Coloration and Polymer Science*, *18*(1), 33-43. https://doi.org/10.21608/jtcps.2021.67798.1050

Guruvenket, S., Andrie, S., Simon, M., Johnson, K. W., & Sailer, R. A. (2012). Atmospheric-pressure plasma-enhanced chemical vapor deposition of a-SiCN: H films: role of precursors on the film growth and properties. *ACS Applied Materials & Interfaces*, *4*(10), 5293-5299. https://doi.org/10.1021/am301157p

Ibrahim, N. A., & Eid, B. M. (2020). Plasma treatment technology for surface modification and functionalization of cellulosic fabrics. *Advances in functional finishing of textiles*, 275-287. https://doi.org/10.1007/978-981-15-3669-4_12

Jaritz, M., Alizadeh, P., Wilski, S., Kleines, L., & Dahlmann, R. (2021). Comparison of HMDSO and HMDSN as precursors for high-barrier plasma-polymerized multilayer coating systems on polyethylene terephthalate films. *Plasma processes and polymers*, *18*(8), 2100018. https://doi.org/10.1002/ppap.202100018

Kim, T. N. T., Vu Thi Hong, K., Vu Thi, N., & Vu Manh, H. (2021). The effect of DBD plasma activation time on the dyeability of woven polyester fabric with disperse dye. *Polymers*, *13*(9), 1434. https://doi.org/10.3390/polym13091434

Kodaira, F. V. P., Mota, R. P., & Moreira Jr, P. W. P. (2015). Thin films growth by PIIID technique from hexamethyldisilazane/argon mixture. *Surface and Coatings Technology*, *284*, 400-403. https://doi.org/10.1016/j.surfcoat.2015.09.063

Kodaira, F. V. P., Mota, R. P., Hills, V. A., Honda, R. I., Kayama, M. E., Kostov, K. G., & Algatti, M. A. (2012). Thin films generated by plasma immersion ion implantation and deposition of hexamethyldisilazane mixed with nitrogen in different proportions. In *Journal of Physics: Conference Series* (Vol. 370, No. 1, p. 012028). IOP Publishing. https://doi.org/10.1088/1742-6596/370/1/012028

Kozak, A. O., Ivashchenko, V. I., Porada, O. K., Ivashchenko, L. A., Tomila, T. V., Manjara, V. S., & Klishevych, G. V. (2018). Structural, optoelectronic and mechanical properties of PECVD Si-CN films: An effect of substrate bias. *Materials science in semiconductor processing*, *88*, 65-72. https://doi.org/10.1016/j.mssp.2018.07.023

Mohamed, H., & El-halwagy, A. A. (2021). Plasma-based Nanotechnology for Textile Coating. *Journal of Textiles, Coloration and Polymer Science*, *18*(1), 11-31. http://doi.org/10.21608/JTCPS.2021.67022.1049

Mourya, S., Jaiswal, J., Malik, G., Kumar, B., & Chandra, R. (2018). Structural and optical characteristics of in-situ sputtered highly oriented 15R-SiC thin films on different substrates. *Journal of Applied Physics*, *123*(2). https://doi.org/10.1063/1.5006976

Murbat, H. H., Abdalameer, N. K., & Brrd, A. K. (2018). Effects of non-thermal argon plasma produced at atmospheric pressure on the optical properties of CdO thin films. *Baghdad Science Journal*, *15*(2), 0221-0221. http://dx.doi.org/10.21123/bsj.2018.15.2.0221

Naebe, M., Haque, A. N. M. A., & Haji, A. (2022). Plasma-assisted antimicrobial finishing of textiles: A review. *Engineering*, *12*, 145-163. https://doi.org/10.1016/j.eng.2021.01.011

Nandiyanto, A. B. D., Oktiani, R., & Ragadhita, R. (2019). How to read and interpret FTIR spectroscope of organic material. *Indonesian Journal of Science and Technology*, *4*(1), 97-118. https://ejournal.kjpupi.id/index.php/ijost/article/view/189

Prado, M., Marski, S. R. D. S., Pacheco, L. P., da Costa Barros, A. W., Gerardo, C. F., Prado, M. C., ... & Simão, R. A. (2022). Hexamethyldisiloxane coating by plasma to create a superhydrophobic surface for fabric masks. *Journal of Materials Research and Technology*, *17*, 913-924. https://doi.org/10.1016/j.jmrt.2022.01.003

Rosace, G., Canton, R., & Colleoni, C. (2010). Plasma enhanced CVD of SiOxCyHz thin film on different textile fabrics: Influence of exposure time on the abrasion resistance and mechanical properties. *Applied Surface Science*, *256*(8), 2509-2516. https://doi.org/10.1016/j.apsusc.2009.10.097

Saloum, S., Abou Shaker, S., Alkafri, M. N., Obaid, A., & Hussin, R. (2019a). Effect of surface modification on the properties of plasma-polymerized hexamethyldisiloxane thin films. *Surface and Interface Analysis*, *51*(7), 754-762. https://doi.org/10.1002/sia.6646

Saloum, S., Shaker, S. A., Hussin, R., Obaid, A., & Alkafri, M. N. (2019b). Plasma CVD/etching of Poly (methyl methacrylate) surface: optical and structural characterizations. *Materials Research Express*, *6*(10), 105371. http://dx.doi.org/10.1088/2053-1591/ab42b1

Saloum, S., Shaker, S. A., Alkafri, M. N., Obaid, A., & Hussin, R. (2020a). Hydrogenated Silicon Carbonitride Thin Film Nanostructuring Using SF 6 Plasma: Structural and Optical Analysis. *Silicon*, *12*, 2957-2966. https://doi.org/10.1007/s12633-020-00392-7

Saloum, S., Shaker, S. A., Hussin, R., Obaid, A., & Alkafri, M. N. (2020b). Effect of atmospheric ageing on the properties of organosilicon (Pp-HMDSO) thin films. *Silicon*, *12*, 1839-1846. https://doi.org/10.1007/s12633-019-00276-5

Samanta, K. K., Joshi, A. G., Jassal, M., & Agrawal, A. K. (2021). Hydrophobic functionalization of cellulosic substrate by tetrafluoroethane dielectric barrier discharge plasma at atmospheric pressure. *Carbohydrate Polymers*, *253*, 117272. https://doi.org/10.1016/j.carbpol.2020.117272

Sohbatzadeh, F., Farhadi, M., & Shakerinasab, E. (2019). A new DBD apparatus for super-hydrophobic coating deposition on cotton fabric. *Surface and Coatings Technology*, *374*, 944-956. https://doi.org/10.1016/j.surfcoat.2019.06.086

Su, T., Han, Y., Liu, H., Li, L., Zhang, Z., & Li, Z. (2019). The surface modification by O2 low temperature plasma to improve dyeing properties of Rex rabbit fibers. *Journal of Engineered Fibers and Fabrics*, *14*, 1558925019854024. https://doi.org/10.1177/1558925019854024

Xu, L., Lai, Y., Liu, L., Yang, L., Guo, Y., Chang, X., ... & Yu, J. (2020). The effect of plasma electron temperature on the surface properties of super-hydrophobic cotton fabrics. *Coatings*, *10*(2), 160. https://doi.org/10.3390/coatings10020160

Zaidy, S. S., Vacchi, F. I., Umbuzeiro, G. A., & Freeman, H. S. (2019). Approach to waterless dyeing of textile substrates—use of atmospheric plasma. *Industrial & Engineering Chemistry Research*, *58*(40), 18478-18487. https://doi.org/10.1021/acs.iecr.9b01260

Zouari, R., Visileanu, E., & Gargoubi, S. (2021). Effect of plasma grafting with Hexamethyldisiloxane on comfort and flame resistance of cotton fabric. *Industria Textila*, *72*(2), 225-230. https://doi.org/10.35530/IT.072.02.1842